===== **MINERALOGY** =====

Bauxites of the Tatarka Deposit (Yenisei Ridge, Russia): The First Evidence of a Contact-Karst Origin

N. M. Boeva[a],*, A. D. Slukin[a], M. A. Makarova[a], E. S. Shipilova[a], Ph. P. Melnikov[a],
D. A. Vnuchkov[a], E. A. Zhegallo[b], L.V. Zaitseva[b], and Academician N. S. Bortnikov[b]

Abstract—The Tatarka bauxite deposit on the territory of the Russian Federation was formed as a result of sedimentation of the products of denuded lateritic weathering crusts of amphibolites in contact-karst depressions. Detailed mineralogical studies of bauxites made it possible to reconstruct reliably the conditions for their formation. As it turned out, the initial rocks and rocks, weathered before, have been denuded due to the close location of the areas of alimentation and accumulation. At the same time, chemical processes have been continued in karst depressions. For the first time, the presence of nanoparticles of amorphous aluminum oxide was revealed in contact-karst bauxites. This specific feature of the form of alumina precipitation is associated with the subsequent cessation of lateritization and their attenuation with depth. The presence of amorphous aluminum monohydrate must be taken into account when choosing a scheme for bauxite enrichment.

INTRODUCTION

Bauxite is known as the primary raw material for aluminum. It is usually formed by intense chemical weathering in hot and humid zones. Bauxite reserves in the world reach several tens of billions of tons. Russia is one of the few countries importing bauxite or alumina to operate aluminum smelters. The potential of the Siberian region, associated with high alumina rocks, has again attracted the attention of researchers because of the Boguchany aluminum smelter placed in operation in Krasnoyarsk krai. Along with sedimentary lateritic bauxites [1, 2], karst depressions filled with scarce bauxite raw materials are of undoubted interest. According to the published data, the bauxite reserves of the Lower Angara region are estimated at 300 million tons of raw materials [3].

Three main genetic types of bauxites are generally recognized: lateritic bauxites obtained as a result of *in situ* lateritization of the underlying aluminosilicate rocks; Tikhvin-type bauxites, which are the products of erosion of pre-existing lateritic bauxites and occur on the eroded surface of aluminosilicate rocks; and karst bauxites developed on the eroded surface of carbonate bedrock. D. Bardoshshi distinguishes the following types of karst bauxites: Mediterranean, Timan, Kazakhstan, Aryezh, Salentine, and Tula [4]. Among the Siberian deposits, there are four morphogenetic types of occurrences: cockpit-type contact-karst as ravine- or canyon-like, ribbon-shaped, and valley-shaped, as well as occurrences of complex karst basins [5]. Contact-carst type of bauxites characterized by an exceptional depth (up to 260 m), far exceeding the depth of the classical karst of the Mediterranean type. Deposits of the region are closest to the type from Kazakhstan; they are characterized by the fact that the carbonate basement is overlapped by a bauxite-bearing formation with a lithologically different, but a genetically unified structure.

Karst-type bauxite ores are typically enriched in many economically important (critical) elements such as V, Cr, Co, Ni, Nb, and REEs [6]. Therefore, it is not surprising that the literature on bauxite deposits has focused on the genetic mechanisms contributing to the formation of this type of sedimentary rocks [6, 7].

Different hypotheses on the formation of bauxites of the contact-karst type have been expressed, such as post-sedimentation, both mechano-clastic [8] and clastogenic formations [9]; authigenic; explosive origin [10]; and hydrothermal-sedimentary [11].

[a] Institute of Geology of Ore Deposits, Petrography, Mineralogy, and Geochemistry, Russian Academy of Sciences, Moscow, 119017 Russia
[b] Borissiak Paleontological Institute, Russian Academy of Sciences, Moscow, 117647 Russia
*e-mail: boeva@igem.ru

The discussion on the origin of contact-karst deposits in Siberia concerns next: whether denudation of already lateritized rocks occurred or whether amphibolite clasts were lateritized after they were moved into karst sinkholes. It remains unclear whether or not denuded weathering products are preserved in karst depressions and whether or not chemical processes cease or continue in them.

To clarify the controversial questions about the mechanisms and stages of the formation of contact-karst bauxites, we studied the chemical and mineral compositions of bauxites and the crystallomorphological features of newly formed and relict rock-forming minerals from bauxites of the Tatarka deposit. This deposit is located in the upper reaches of the Tatarka River and occupies an erosion-tectonic basin at 350–450 m a.s.l., framed by the heights of the Tatarka Ridge (up to 800 m) to the north, west, and south, and by the swells of the Tatarka granite massif (up to 650 m) to the east [9].

GEOLOGICAL STRUCTURE OF THE TATARKA DEPOSIT

Bauxite deposits are attributed to the Central anticlinorium of the Yenisei Ridge composed of Precambrian carbonate−terrigenous rocks. The rocks are extremely dislocated, metamorphosed, and broken by acidic and mafic intrusions [5]. In many of them, lateritic weathering crusts were developed and, in places, were preserved in the depressions with a steep fall of limestones and along subvertical contacts with other rocks, deep karst develops. Most of them, especially the upper horizons, were eroded and redeposited as bauxite-bearing sediments. The Paleocene−Eocene age (Murozhkoi Formation) of the rocks was determined on the basis of the spore−pollen analysis [9]. This formation is associated with several groups of bauxite deposits concentrated in three regions: in the Central anticlinorium, on the eastern margin, and on the southeastern part of the ridge.

Bauxites occur in karst sinkholes extending in the form of a chain along a strike of limestones or along the contact between the latter and amphibolites. The size of V-shaped karst depressions reaches 500×250 m, and the depth is up to 260 m, i.e., slightly below the modern hydrographic network (Fig. 1a).

The deposit is composed of Middle Proterozoic dislocated limestones, quartzites, and phyllites. Crosscutting and bedded bodies of amphibolites are widely developed. In the Tatarka Basin, weathering crusts were developed on these rocks. The weathering crusts are overlapped by Paleocene−Eocene bauxite-bearing sediments, which are preserved in karst depressions of some deposits. Clays and bauxites predominate in the central part of the basin, while sandy and sandy−clayey sediments with bauxites containing fragments of weathered and lateritized amphibolites

prevail at the margins. The weathering crust, crowned by a kaolinite zone, remains preserved on amphibolites (Fig. 1b).

The Tatarka deposit consists of 12 ore bodies filling karst sinkholes and of two bodies in the remnants of the ancient valleys. The karst depressions are filled with Paleocene−Eocene bauxite-bearing sediments. From one to three ore horizons are distinguished: from bottom to top, brown sandy kaolinite clays are replaced by variegated clays, bauxite clays and bleached bauxites, and, finally, by coaly clays and coals with abundant fragments and concretions of rocky bauxite [5]. Rocky or vermicular bauxites are generally found in the upper parts of bauxite-bearing sediments, while clayey ones are located in the lower, deepest part. Large fragments of fresh, weathered, and fully lateritic amphibolites have been identified in the bauxites. Loose and clayey bauxites accounting for 47.4 and 40.4% of the deposit reserves, respectively, play the main role in the ores [9].

METHODS

About 30 samples of bauxite and associated rocks from boreholes and outcrops of the Tatarka deposit were collected and studied.

The chemical composition of bauxite was determined using the Axios "RANalytical" X-ray fluorescence spectrometer.

The mineral composition was studied by X-ray phase analysis (XRF) on an Ultima-IV Rigaku diffractometer, by synchronous thermal analysis (STA), and with the help of the Cambridge CamScan 4 and Tescan TESCAN VEGA IIXMU scanning microscopes (SEM) with the energy dispersive attachment (EDS).

The STA was conducted on an instrument (STA 449 F1 Jupiter Netzsch). Shooting was performed at a rate of $10°/min$ in the air atmosphere in crucibles with closed lids to a temperature of $1050°C$. The mass of the sample weight was ~40 mg.

RESULTS

Chemical Composition

Rocky, loose, and clayey rocks of the Tatarka deposit were analyzed.

The Al_2O_3 content in rocky or vermicular bauxite ranges from 41.44 to 59.45 wt %, with an average of 50.6 wt %. The SiO_2 content varies from 1.48 to 7.97 wt %, with an average of 3.3 wt %. The TiO_2 values vary from 1.17 to 4.08 wt %, with an average of 2.9 wt %. The Fe_2O_3 content varies quite widely from 6.86 to 34.05 wt %, averaging 19.62 wt %. The content of Na_2O varies from 0.05 to 0.39 wt %, CaO from 0.01 to 0.4 wt %, MnO from 0.02 to 0.04 wt %, P_2O_5 from 0.08 to 0.3 wt %, and MgO from 0.01 to1.28 wt %. In comparison with other samples investigated, high Cr
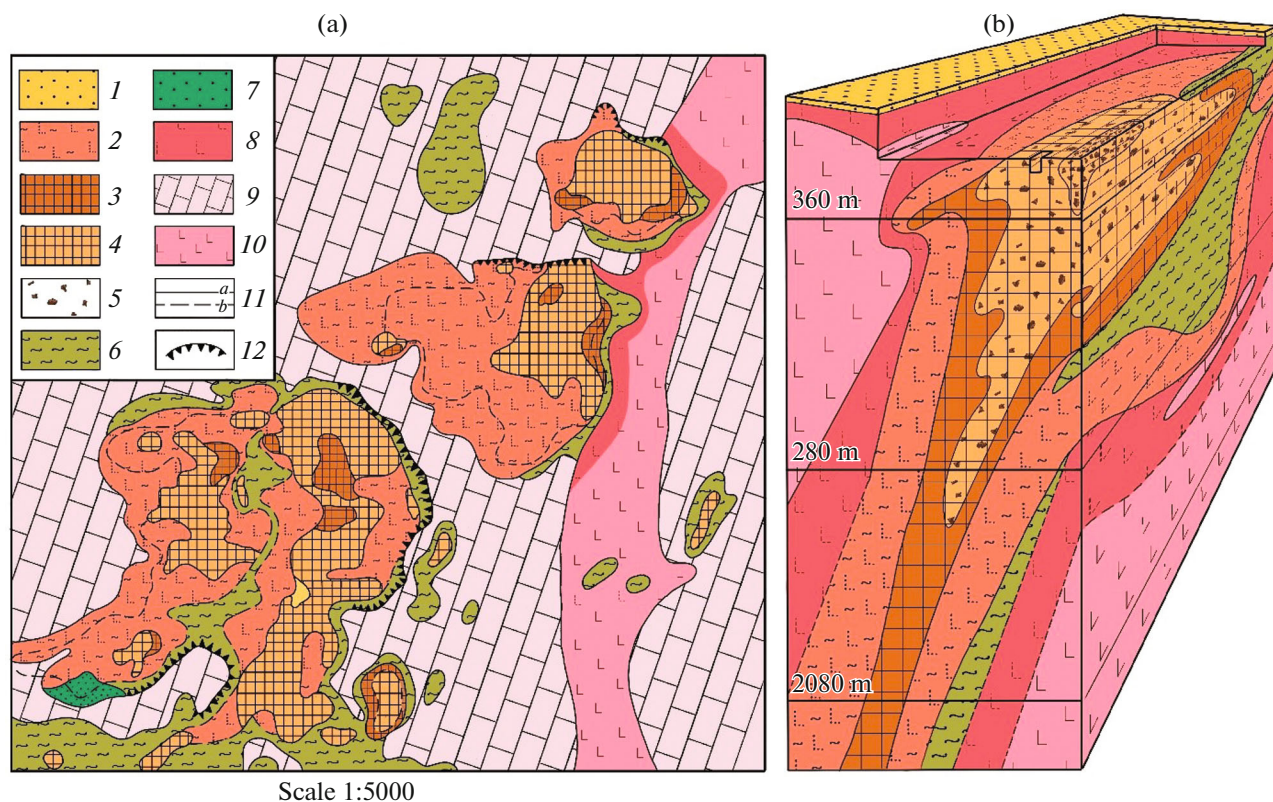
Fig. 1. Geological map of the central part of the Tatarka bauxite deposit, Yenisei Ridge (according to E.I. Peltek [9]), and (a) the prospective block diagram of ore body 9 (according to R.A. Tsykin [12]) (b) with additions. Quaternary sediments: (*1*) cover loams and clays; Paleogene sediments of the Murozhkoi Formation (productive sub-formation): (*2*) mottled kaolinite clays, (*3*) clayey bauxite, (*4*) loose bauxite, (*5*) rocky bauxite, (*6*) brecciated clays and silty-clay deposits with fragments of basement rocks and bauxites, (*7*) calcareous quartz sand; (*8*) weathering crust of amphibolites; Proterozoic sediments: (*9*) limestones; the Proterozoic Indyglin intrusive complex: (*10*) amphibolites, (*11a*) rock boundaries, (*11b*) contours of buried ore bodies, and (*12*) ledges of karst relief.

contents from 570 to 1238 g/t, on average 938 g/t, were determined in rocky bauxite.

The Al_2O_3 content in loose bauxites varies from 33.5 to 56.35 wt %, averaging 44.2 wt %. In this group of samples, there is a reduced water content, which does not correspond to the composition of aluminum trihydrate. The SiO_2 values vary from 0.87 to 9.18 wt %; TiO_2, from 1.79 to 8.07 wt %; Fe_2O_3, from 10.09 to 42.42 wt %, averaging 32.67 wt %; Na_2O, from 0.07 to 0.3 wt %; Ka_2O, from 0.03 to 0.05 wt %; CaO, from 0.02 to 0.3 wt %; MnO, from 0.01 to 0.13 wt %; and P_2O_5, from 0.1 to 0.39 wt %. Increased values of V and Nb from 509 to 946 g/t and from 95 to 180 g/t, respectively, are noted in loose bauxite in comparison with other samples.

The Al_2O_3 content in the clayey rocks ranges from 15.89 to 26.29 wt %, with an average of 22.75 wt %. The SiO_2 values vary from 36.89 to 46.6 wt %, averaging 41.21 wt %. The TiO_2 contents vary from 1.58 to 7.2 wt %, averaging 3.59 wt%. The Fe_2O_3 content varies from 14.02 to 17.08 wt %, with an average of 16.05 wt %. The content of other components is as fol-

lows: Na_2O, from 0.1 to 0.5 wt %; K_2O, from 0.07 to 0.16 wt %; CaO, from 2.9 to 6.56 wt %; and P_2O_5, from 0.11 to 0.21 wt %. Higher contents of Ni, Cu, Zn, and Ba were determined in the samples compared to others. This is due to the excellent sorption properties of clayey rocks. The metal contents are the following: Ni from 95 to 254 g/t, Cu from 332 to 914 g/t, Zn from 125 to 401 g/t, and Ba from 195 to 672 g/t.

However, according to XRF analysis, some samples had a higher concentration of alumina than its content in gibbsite.

X-ray Phase Analysis

The results of X-ray phase analysis are presented in Table 2 and Fig. 2. The main minerals in all bauxite samples are gibbsite, hematite, and goethite. In addition to them, quartz, anatase, kaolinite, montmorillonite, ilmenite, rutile, plagioclase, tourmaline, and hornblende were found in the studied samples. The minerals were identified according to the most important and typical interplanar distances: 4.82 and 4.34 Å for gibbsite; 4.18, 2.69, and 2.45 Å for goethite;

Table 1. Chemical composition of bauxites of the Tatarka deposit

Sample	LOI	Na$_2$O	MgO	Al$_2$O$_3$	SiO$_2$	K$_2$O	CaO	TiO$_2$	MnO	Fe$_2$O$_3$	P$_2$O$_5$	S	Cr	V	Co	Ni	Cu	Zn	Ba	Nb
	wt %	wt %	wt %	wt %	wt %	wt %	wt %	wt %	wt %	wt %	wt %	wt %	g/t	g/t	g/t	g/t	g/t	g/t	g/t	g/t
Rocky bauxites																				
12/75	26.10	0.08	0.04	54.65	3.19	0.04	0.02	4.08	0.044	11.08	0.25	<0.02	1238	475	29	31	85	26	<10	68
12/2	27.71	0.05	0.01	55.35	1.48	0	<0.01	1.17	0.02	13.41	0.08	<0.02	570	314	33	22	114	121	11	16
11	28.37	0.07	0.00	59.45	1.51	0.04	0.02	2.89	0.028	6.86	0.30	<0.02	1095	449	27	18	57	19	41	54
09/75	11.75	0.39	1.28	42.09	7.97	0.03	0.41	2.82	0.033	32.71	0.16	0.04	704	468	46	117	68	63	15	28
10/75	17.60	0.07	0.05	41.44	2.44	0.03	0.03	3.59	0.047	34.05	0.25	0.04	1083	711	72	24	89	49	25	47
Loose bauxites																				
04/74	16.28	0.17	0.47	43.75	2.93	0.04	0.15	3.33	0.047	32.37	0.11	0.03	347	658	69	13	154	51	22	95
01/74	13.06	0.08	0.05	43.98	1.19	0.03	0.04	3.65	0.038	37.36	0.14	0.04	477	640	42	<10	76	37	23	154
11/75	19.99	0.30	1.16	56.35	9.18	0.05	0.32	1.79	0.013	10.09	0.39	0.02	975	509	32	14	73	52	31	47
06/74	11.54	0.23	0.62	43.59	3.60	0.03	0.15	3.20	0.037	36.44	0.13	0.04	709	647	59	39	91	49	11	123
08/74	15.05	0.08	0.04	43.88	1.13	0.03	0.04	4.38	0.038	34.85	0.10	0.04	414	660	44	14	97	42	15	180
09/74	13.93	0.07	0.04	33.50	1.02	0.03	0.02	8.07	0.131	42.42	0.22	0.07	448	946	41	21	339	115	30	105
3T	14.80	0.07	0.02	44.37	0.87	0.03	0.02	4.14	0.042	35.15	0.11	0.03	419	640	49	<10	99	34	16	165
Clayey rocks																				
15/74	6.41	0.53	3.70	26.17	36.89	0.16	6.56	1.58	0.231	17.05	0.16	<0.02	268	329	80	254	332	125	366	8
18/74	7.98	0.10	1.31	15.89	46.60	0.07	2.90	7.20	0.161	17.08	0.21	<0.02	100	637	60	95	914	149	195	42
19/74	11.11	0.11	1.67	26.19	40.15	0.11	3.81	2.00	0.303	14.02	0.11	<0.02	68	325	49	193	590	401	672	15

Table 2. Mineral composition of karst bauxite and clayey rocks from the Tatarka deposit (wt %)

Sample	Smectite	Kaolinite	Quartz	Plagioclase	Hornblende	Tourmaline	Anatase	Ilmenite	Rutile	Goethite	Hematite	Gibbsite	X-ray phase
-Rocky bauxites													
12/75	N/D	N/D	3	N/D	N/D	N/D	11	N/D	N/D	5	6	75	N/D
12/2	N/D	N/D	1	N/D	N/D	N/D	1	N/D	N/D	5	8	85	N/D
11	N/D	N/D	N/D	N/D	N/D	N/D	3	N/D	N/D	3	3	91	N/D
9/75	N/D	N/D	2	1	N/D	15	N/D	N/D	N/D	10	21	48	3
10/75	N/D	N/D	N/D	N/D	N/D	N/D	3	N/D	N/D	10	24	55	8
-Loose bauxites													
4/74	N/D	N/D	N/D	N/D	N/D	3	3	N/D	N/D	N/D	32	50	12
1/74	N/D	N/D	N/D	N/D	N/D	N/D	3	N/D	N/D	N/D	37	35	25
11/75	N/D	1	2	6	N/D	9	N/D	N/D	N/D	5	5	52	20
6/74	N/D	N/D	2	N/D	N/D	5	1	N/D	2	N/D	34	32	24
8/74	N/D	N/D	N/D	N/D	N/D	N/D	4	N/D	N/D	N/D	34	43	19
9/74	N/D	N/D	1	N/D	N/D	N/D	N/D	6	2	16	27	30	18
3T	N/D	N/D	N/D	N/D	N/D	N/D	4	N/D	N/D	N/D	35	43	18
-Clayey rocks													
19/74	20	39	11	2	6	N/D	N/D	N/D	2	11	4	5	N/D

2.69, 1.69, and 2.51 Å for hematite; 3.34, 4.25, and 1.81 Å for quartz; 3.51, 1.89, and 2.37 Å for anatase; 7.13, 1.49, and 3.56 Å for kaolinite; 11.5, 1.49, and 4.45 Å for montmorillonite; 2.74, 2.53, and 1.72 Å for ilmenite; 1.68, 3.24, and 2.48 Å for rutile; 2.95, 3.18, and 4.03 Å for plagioclase; 2.59, 4.48, and 6.5 Å for tourmaline; and 1.05, 1.44, and 2.71 Å for hornblende.

The results of X-ray phase analysis provided insight into the overestimated alumina content. Due to the fact that no other aluminum-bearing minerals have been detected in the bauxites, it is assumed that X-ray amorphous aluminum oxide is present. Thus, for the first time in the bauxites of Yenisei Ridge, an excessive alumina content was detected in the samples compared to gibbsite due to an admixture of the X-ray amorphous phase containing aluminum.

Synchronous thermal analysis of the studied samples allowed us to determine the influence of the structural features and the particle size of gibbsite on the character of the obtained curves. Gibbsite distinctly differs from sedimentary bauxite by the absence of additional endo-effects on the differential scanning
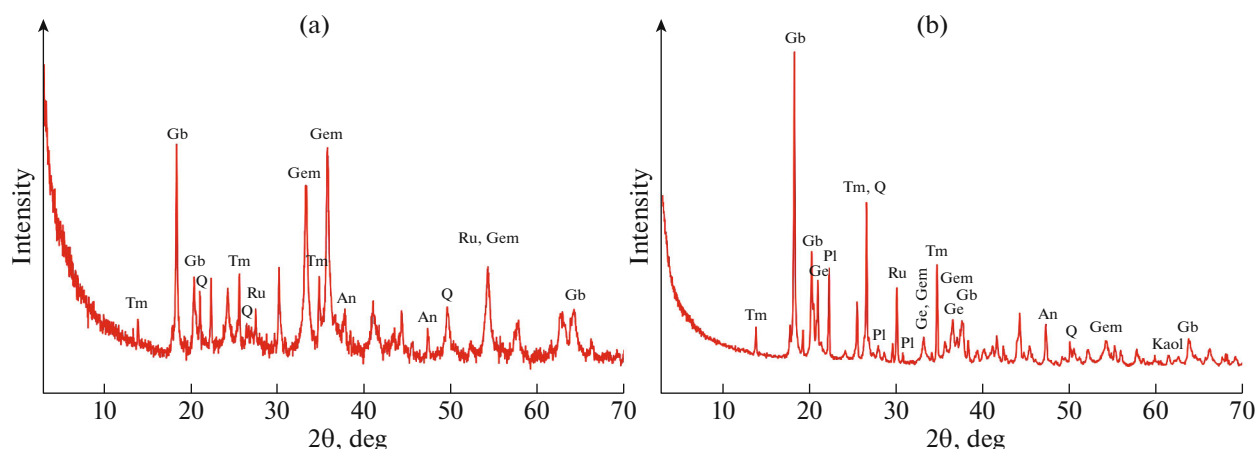

Fig. 2. X-ray diagrams of bauxite: (a) sample 06/74, (b) sample 11/75. Gb, gibbsite; Ge, goethite; He, hematite; An, anatase; Ru, rutile; Tm, tourmaline; Q, quartz; Kaol, kaolinite; and Pl, plagioclase.
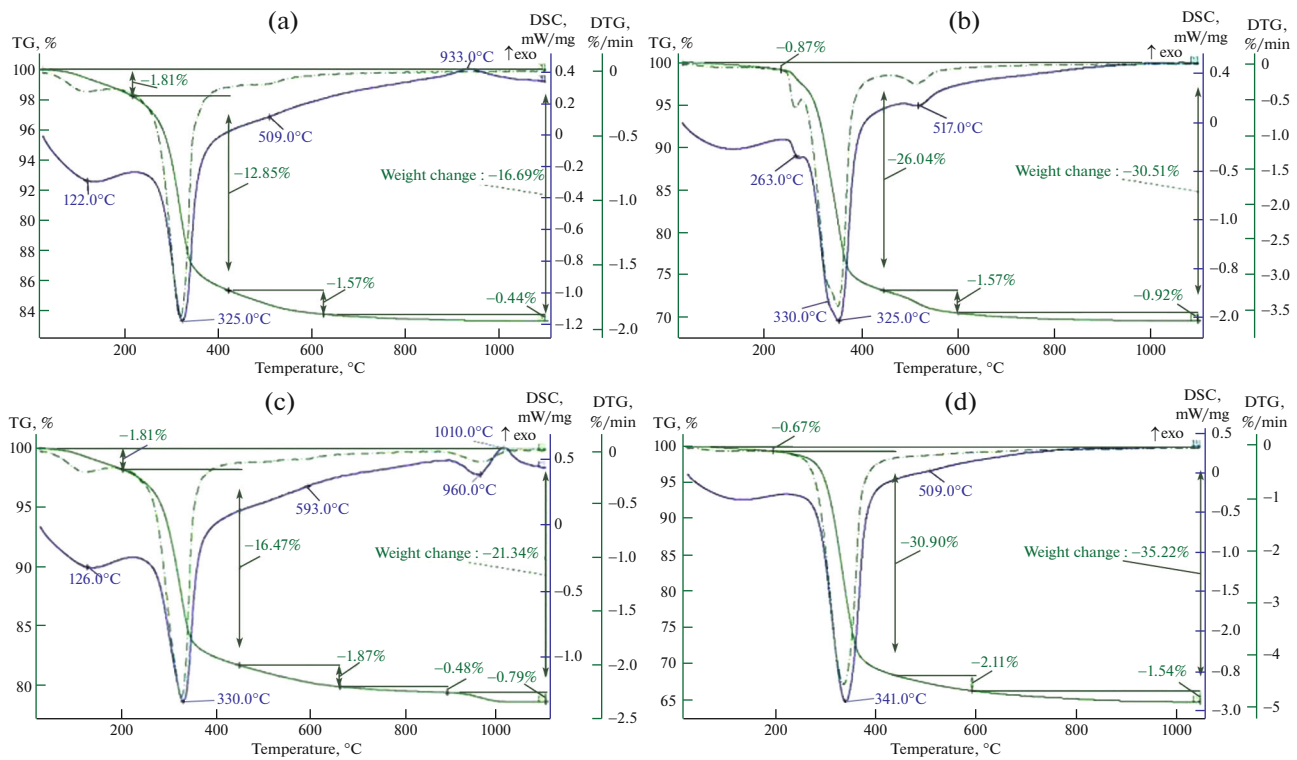
Fig. 3. Thermal curves of bauxite: (a) sample 3T, (b) sample 12T/3, (c) sample11/75, (d) sample 6T.

calorimetry (DSC) curves in the interval of dehydroxylation of the mineral (250–400°C), which we observe in most samples (Fig. 3a). However, there are samples, taken from the central parts of the large samples, in which the DSC plots show step-by-step dehydroxylation of a mineral associated with a large size of gibbsite crystals, typical of minerals formed exclusively in situ (Fig. 3b). In some samples, the presence of tourmaline was detected, the dissociation of which is displayed as an endo-effect on the DSC curve in the temperature range 900–1050°C (Fig. 3c). The exo-effect at 1050–1200°C is responsible for the transition of γ-Al_2O_3 to α-Al_2O_3. Figure 3d shows the thermal curve of gibbsite with a single maximum at 341°C. The endo-effect has a regular shape typical of gibbsite crystals with an ordered structure [13, 14] formed by biofilms in the process of lateritization continuing after denudation (Fig. 4g).

The quantitative ratio of minerals in bauxite can be determined only by comparison of three methods, that is, X-ray fluorescence, X-ray phase, and thermal: the gibbsite content ranges from 30 to 90 wt %; X-ray amorphous aluminum oxide, from 3 to 25 wt %; hematite, from 14 to 57 wt %; and goethite, from 6 to 22 wt %. Minerals characteristic of the bedrocks—amphibolites—are also present: plagioclase, hornblende, and tourmaline. The results are summarized in Table 2.

Scanning Electron Microscopy

The SEM shows that abundant pores, caverns, and wood debris are present in the fine-grained clay matrix. The pore outlines are characterized by triangular, prismatic shapes indicating quartz dissolution. Square and diamond shapes are traces of dissolved calcite grains. The phytomorphoses are ferruginous and have well-traced hematite biomorphoses by bacteria (Figs. 4a, 4b). The SEM allowed us to establish the morphology of crystals. Fresh idiomorphic crystals of amphiboles and feldspars are well preserved primary forms (Fig. 4c). In some crystals there are caverns made by druses of gibbsite crystals (Fig. 4d). Newly formed gibbsite grains are also observed on the crystal surface. The matrix in the interstices between amphibole crystals is replaced by a mixture of kaolinite and gibbsite. Finally, areas of amphibolites completely replaced by gibbsite are observed.

In sedimentary bauxite, in a highly dispersed medium, caverns are found. Newly formed hemispherical precipitates of tabular gibbsite crystals are developed on the walls of the caverns. Crusts of short-prismatic gibbsite crystals are revealed on the surfaces of the small nodules (Fig. 4e).

Large relict crystals of ilmenite, well preserved in their shape, are found in the fine-grained matrix. In the chemical composition of ilmenite, there is a significant (up to 4 wt %) impurity of V (Fig. 4f). Quartz, anatase, and rutile—relict minerals of amphibolites—
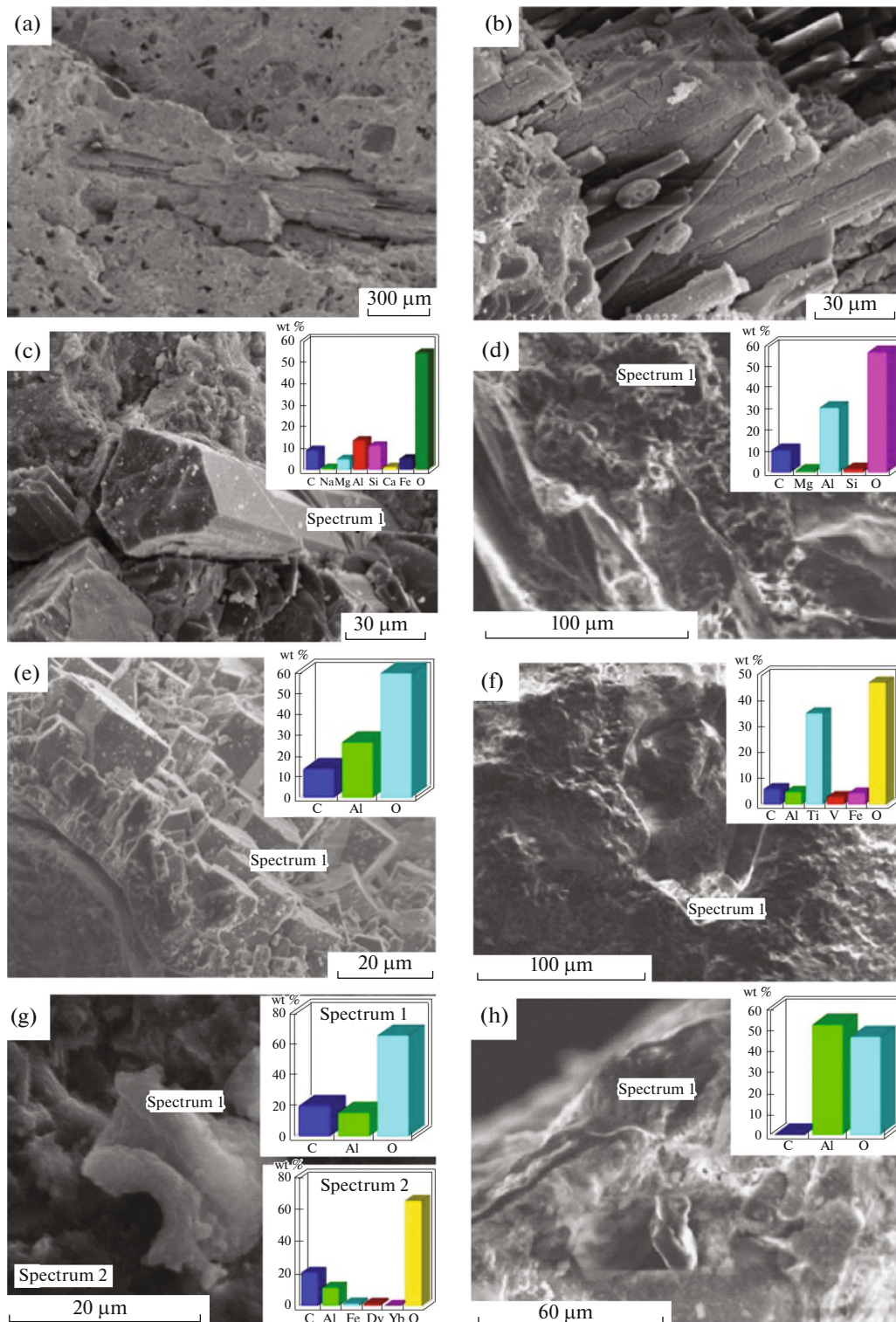
Fig. 4. (a) Fine-grained clayey matrix of bauxites, (b) phytomorphoses on wood and biomorphoses on bacteria, (c) idiomorphic crystals of amphiboles, (d) caverns made by druses of gibbsite crystals, (e) crusts of short prismatic gibbsite crystals, (f) ilmenite crystal, (g) biofilms of complex composition, biogenic gibbsite, and (h) amorphous aluminum hydroxide SEM. EDS of composition.

were also detected. Their content varies within a percentage point. It should be emphasized that part of the titanium is not associated with these minerals, but is sorbed by biofilms. All minerals of lateritized amphibolites have no traces of mechanical movement; i.e., they all occur in situ. Remnants of incompletely dis-

solved calcite grains are occasionally found in bauxites. Sedimentary bauxites are abundantly penetrated by biomineral films. They have a diverse appearance. They can occur in the form of thin covers of fluffy snow-like deposits. Their chemical composition is very diverse. Biogenic gibbsite is formed on aluminum films. Gibbsite with Fe, Dy, and Yb impurities is formed on the films of more complex composition (Fig. 4g). Hematite is in the form of ochre pseudomorphoses on amphiboles, as well as in the form of framework crystal lattices, biomorphoses, and uncrystallized biomineral films. Uncrystallized aluminum biofilms lose water and form X-ray amorphous aluminum oxide (Fig. 4h).

DISCUSSION

The results obtained allowed us to conclude that the Tatarka bauxite deposit occurred as a result of the sedimentation of the denudated lateritic bauxite formed on amphibolites and other rocks in the contact-karst depressions.

In the area of the Tatarka deposit, in the Cretaceous−Paleogene time, there were conditions under which the bedrocks—amphibolites and products of their redeposition, represented by large fragments of weathered and lateritized amphibolites in contact-karst bauxites—occurred in close proximity. Due to such proximity and steep contacts of weathered amphibolites and limestones, a number of specific features were manifested in the disintegration, denudation, and accumulation. Thus, fragments of pseudomorph bauxites, even 1−2 cm in size, are very rarely found in all bauxites of karst and erosional depressions on the neighboring Siberian Platform. In the bauxites of the Tatarka deposit, such fragments even greater than 10 cm in size are abundant [15]. Fragments of tree trunks and branches with hematite biomorphoses are mixed with them (Figs. 4a, 4b). This indicates a very short transportation path of denuded amphibolites to the basin of their accumulation in karst depressions. Large fragments of fresh and weathered amphibolites retain textural and structural features of the primary rocks formed in situ.

Idiomorphic crystals of amphiboles were detected among them (Fig. 4c). The DSC plots demonstrate additional endo-effects in the dehydroxylation interval (Fig. 3b), indicating that the formation of gibbsite in the rock occurred in situ before it was moved into the karst depression. The preserved gibbsite crystals are evidence of the close contact between products from the areas of alimentation and accumulation. Gibbsite is the main mineral of lateritized amphibolites. Its content in some samples reaches 91 wt %. It is found in the form of pseudomorphoses of hexagonal tabular crystals replacing feldspars and amphiboles; in the form of druses of tabular, prismatic, and pyramidal crystals in caverns and fractures; and in the form of hidden crystalline nest-like precipitations. The content of gibbsite in bauxite decreases with depth.

After denudation and accumulation into karst depressions, the sediment is transformed. The electron microscope clearly shows that the dispersed particles of the fine bauxite matrix are in a close disorderly mixture (Fig. 4a). Numerous caverns, cracks, and many passages of burrowing organisms are formed; chemically and biochemically active waters are filtered through them. Rainwater is enriched with organic acids penetrating to depth through the cracks, dissolving fine minerals. Surface and underground karst watercourses also participate in the transformation of bauxite [15].

Dissolved alumina is released in large fractures in the form of crusts and druses of gibbsite crystals. It dissolves and crystallizes again in the fine-grained matrix, then cladding nodules and cavern walls (Fig. 4e). The presence of biogenic gibbsite is confirmed by thermal analysis (Fig. 3d). The endo-effect on the DSC curve has a shape typical of gibbsite crystals with an ordered structure. At the same time, watered mineral surfaces are covered with abundant biomineral films (Fig. 4g). They have high sorption abilities, enriching bauxite with various chemical elements—Al, Ti, Fe, Dy, Yb, and others. Rare earth elements were input by surface and karst waters from the Tatarka massif of nepheline syenites and manifestations of carbonatites [15]. Thus, we can confirm that lateritization continued after sedimentation.

Subsequently, as a result of the changed conditions, the lateritization process was interrupted and the remaining alumina was preserved as amorphous aluminum monohydrate (Fig. 4g). The Al_2O_3 content significantly exceeds the amount of alumina that can be included in the gibbsite composition, which is clearly reflected in the EDS of the composition (Fig. 4h). As the depth in the karst sinkholes increases, the content of X-ray amorphous aluminum oxide in bauxite increases (Table 2). This is explained by the attenuation of lateritization with depth.

CONCLUSIONS

The studies conducted allowed us to establish reliably the contact-karst origin of the Tatarka deposit and its peculiarities. The main feature is the closest possible location of alimentation and accumulation areas. Fracture products of bedrocks were carried directly into karst depressions. Not only were products of the surface planar denudation carried into them, so were rocks from the vertical outcrops of the weathering crust profile. Thus, proper lateritic bauxites and the underlying rocks were mixed in the ore bodies.

The relict structure of amphibolites is perfectly preserved in weathering products. In sedimentary bauxites, gibbsite is preserved well in fragments of lateritized amphibolites in karst depressions. The fine-

grained matrix mottled with point voids, left in place of dissolved carbonate and quartz grains, as well as the abundance of biomineral films and their crystallization products, is a clear sign of the ongoing weathering typical of lateritization.

The presence of nanoparticles of amorphous aluminum oxide was revealed in contact-karst bauxites. This specific feature of the alumina precipitation form is associated with the termination of the lateritization processes and their attenuation with depth. The presence of amorphous aluminum monohydrate should be taken into consideration when selecting the scheme of bauxite enrichment.

FUNDING

CONFLICT OF INTEREST

The authors declare that they have no conflicts of interest.

OPEN ACCESS

REFERENCES

1. N. M. Boeva, A. D. Slukin, E. S. Shipilova, M. A. Makarova, F. V. Balashov, E. A. Zhegallo, L. V. Zaitseva, and N. S. Bortnikov, Dokl. Earth Sci. **500** (1), 720−728 (2021).

2. N. M. Boeva, M. A. Makarova, E. S. Shipilova, A. D. Slukin, F. P. Mel'nikov, O. V. Karimova, and N. S. Bortnikov, Dokl. Earth Sci. **507** (1), 871−881 (2022).

3. *Mineral Resources of the Krasnoyarsk Territory. Cadastre of Mineral Deposits,* Ed. by S. S. Serdyuk (Krasnoyarsk Res. Inst. Geo. Mineral. Raw Materials, Krasnoyarsk, 2002), Books 1, 2 [in Russian].

4. G. Bardossy, *Karst Bauxites: Bauxite Deposits on Carbonate Rocks* (Elsevier, Amsterdam, 1982).

5. G. R. Kirpal', *Industrial Types of Bauxite Deposits and Their Geological and Economical Estimation* (Nedra, Moscow, 1977) [in Russian].

6. G. Mongelli, M. Boni, G. Oggiano, P. Mameli, R. Sinisi, R. Buccione, and N. Mondillo, Ore Geol. Rev. **86**, 526−536 (2017).

7. S. Yang, Q. Wang, J. Deng, Y. Wang, W. Kang, X. Liu, and Z. Li, Ore Geol. Rev. **115**, 103161 (2019).

8. B. V. Shibistov, *Laterites and Continental Bauxites* (Krasnoyarsk Res. Inst. Geo. Mineral Raw Materials, Krasnoyarsk, 2000) [in Russian].

9. *Platform Bauxites of the USSR,* Ed. by D. G. Sapozhnikova (Nauka, Moscow, 1971) [in Russian].

10. G. N. Cherkasov, in *Coll. Sci. Works Siberian Res. Inst. Geol., Geophys., Miner. Resour. "Problems on Siberian Geology, Ore Formation and Minerageny"* (Novosibirsk, 2000), pp. 29−38 [in Russian].

11. V. N. Razumova, in *Trans. Geol. Inst, USSR Acad. Sci. "Processes of Continental Lithogenesis"* (Nauka, Moscow, 1980), Vol. 350, pp. 60−92 [in Russian].

12. *Tsykin Rostislav Alekseevich: Bibliographical Index,* Ed. by E. A. Naprienko, S. P. Anikin, N. M. Safonov, and V. A. Koreshkov (Siberian Federal Univ., Krasnoyarsk, 2015) [in Russian].

13. N. M. Boeva and N. S. Bortnikov, Dokl. Earth Sci. **510** (1), 525−531 (2023).

14. N. M. Boeva, N. S. Bortnikov, A. D. Slukin, E. S. Shipilova, M. A. Makarova, and F. P. Melnikov, Minerals **11** (11), 1184−1195 (2021).

15. A. D. Slukin, in *Coll. Sci. Works Siberian Res. Inst. Geol., Geophys., Miner. Resour. "Ore-Bearing Karst of the Siberia,"* Novosibirsk, 1989, pp. 22−33 [in Russian].

Translated by V. Krutikova